Adaptive boundary element computation of acoustic radiation and scattering problems in two dimensions

K. H. Chen and J. T. Chen

Department of Harbor and River Engineering, National Taiwan Ocean University, Keelung, Taiwan

Abstract

In this paper we carry out boundary element computations of the Helmholtz equation in two dimensions, in the context of time-harmonic exterior acoustics. The purpose is to demonstrate cost savings engendered through adaptivity for propagating solutions at moderate wave numbers. The computations are performed on meshes of constant boundary elements, and are adapted to the solution by locally changing element sizes (h-version). Burton and Miller approach is employed to solve the exterior problems for all wave numbers. Two error indicators obtained from the dual integral equations in conjuction with the exact error indicator are used for local error estimation, which are essential ingredients for all adaptive mesh schemes in BEM. Computational experiments are performed for the two-dimensional exterior acoustics problems. The three error tracking curves are in good agreement with their shapes. Two examples show that the adaptive mesh based on the error indicators converge faster than does uniform mesh discretization.

Keywords: boundary element, exterior acoustics, adaptivity, error indicators.

自適性邊界元素法在二維輻射與散射聲場之計算

陳桂鴻與陳正宗

海洋大學河海工程學系, 基隆, 臺灣

摘要

本文以邊界元素法求解二維外域聲場問題, 配合 Burton and Miller 法解決了外域聲場數值共振的問題。並使用自適性網格切割的策略將誤差較大的問題邊界重新切割網格, 提高求解的效率。所使用的自適性網格切割策略是屬於h-型。本文所採取的誤差指標爲對偶積分方程式的第一式 (UT) 的殘餘量、第二式 (LM) 的殘餘量與解析差量等三種來作爲局部誤差的估計, 而成爲自適性網格切割的策略的判斷依據。最後以兩個數值算例說明 了使用自適性網格切割將提高解的收斂效率, 驗證本法的可行性。

關鍵字: 邊界元素法, 外域聲場, 自適性網格切割, 誤差指標

1. INTRODUCTION

Numerical methods are always utilized to solve problems especially when an exact solution is not available. The discretization process, which transforms a continuous system into a discrete system using finite number of degrees of freedom, results in errors. The discretization error is defined as a measure of difference between the exact solution and the numerical approximation. Obtaining a reliable error estimation is to guarantee a certain level of accuracy for the numerical results, and is a key factor of the adaptive mesh procedure. Thus, estimation of the discretization error in the numerical method is the first step in adaptive mesh generation.

The h-version, p-version and r-version schemes [1] have been recently used to improve numerical accuracy. In the h-version

scheme, the total number of elements increases, but the order of the interpolation function remains unchanged. Since the global matrix must be reformulated after mesh refinement, the computational cost becomes very high. In this way, the efficient remesh tactics is required when h-version scheme is adopted. The adaptive tactics for h-version are generally referred to as the reference value method [1], in which the element mesh is refined where the error is larger than the prescribed reference value. This provides a criterion to determine where the elements should be divided into more partitions by finding the residuals in the integral equation pointwisely.

A large number of studies on adaptive BEM have been done by Kamiya *et al.* [2], using sample point error estimation. However, the error stems not only from the discretization procedure, but also from the mismatch of the collocation points on the boundary. Zarikian *et al.*[3] and Paulino *et al.* [4] used pointwise error estimation to study the convergency of the interior problem by using the hypersingular residuals. Both the singular integral equation (UT) and hypersingular integral equation (LM) in the dual BEM can independently determine the unknown boundary data for the problems without a degenerate boundary. The residuals obtained from these two equations can be used as indexes of error estimation. This provides a guide for remeshing without the mismatch of the collocation points on the boundary in the sample point error method. By creating more divisions in the boundary mesh where the estimated error is large, the error curve will be redistributed. Therefore, Liang *et al.* [5] applied the hypersigular equation to find the residual for error estimation in the Laplace equation. Both interior and exterior problems were considered.

In studying the exterior acoustics problems as shown in Fig.1(a), finite element method in conjunction with the DtN (Dirichlet to Neumann) technique was found to be competitive [11] in comparison with BEM. Later, adaptive FEM was extended to solve the problems more efficiently [11, 7]. For the practical engineers, BEM is more attractive since the model creation takes a fewer time for one-dimension reduction. The mesh of DtN FEM and the BEM mesh are shown in Figs.1(b) and 1(c), respectively. Although BEM results in fictitious frequency, it can be circumvented by employing the Burton and Miller formulation. Here, we will focus on the adaptive BEM for exterior acoustics problems in two dimensions.

In this paper, the Burton and Miller formulation by combining the dual boundary integral equations is utilized to solve the exterior acoustics problems for all wave numbers in order to avoid the problem of fictitious frequency. Two residuals, derived by the nonzero terms, which are calculated by substituting the boundary data obtained previously from the Burton and Miller method and known boundary data into the sigular and hypersingular integral equations, are found. According to the residuals by collocating the points along the boundary, error tracking curves can be constructed. Numerical examples are performed for two-dimensional exterior acoustics problems to demonstrate the cost effectiveness of adaptive scheme.

2. STATEMENT FOR EXTERIOR BOUNDARY-VALUE PROBLEMS OF THE HELMHOLTZ EQUATION

Let $D \subset D^d$ be an unbounded region, where d is the number of space dimensions, d can be 1, 2 or 3. The boundary of D, denoted by B, is internal and assumed piecewise smooth as shown in Fig.1. The outward unit vector normal to B is denoted by n. We assume that boundary, B, admits the partition

$$B = B_g \cup B_h, \tag{1}$$

$$\phi = B_g \cap B_h. \tag{2}$$

We intend to study the effects of small distrurbances to a given background flow in such a region, under the usual assumptions that led to the equations of acoustics. Harmonic analysis leads to a boundary-value problem for the Helmholtz equation (or reduced wave equation): Find u in the exterior domain, the spatial component for the acoustics pressure or velocity potential, such that

$$-\mathcal{L}u = f \qquad \text{in } D, \tag{3}$$

$$u = g \qquad \text{on } B_g, \tag{4}$$

$$\frac{\partial u}{\partial n} = ikh \qquad \text{on } B_h, \tag{5}$$

$$\lim_{r\to\infty} r^{\frac{1}{2}(d-1)}\left(\frac{\partial u}{\partial r} - iku\right) = 0, \tag{6}$$

where $\mathcal{L}u := \nabla^2 u + k^2 u$ is the Helmholtz operator, ∇^2 is the Laplace operator and $k \geq 0$ is the wave number; an inferior comma denotes partial differentiation, and, in particular $\frac{u}{n} := \nabla u \cdot \mathbf{n}$ is the normal derivative and ∇ is the gradient operator; $i^2 = -1$; r is the distance from the origin; and g and h are the prescribed boundary

data. In the linearized equations of motion, velocity gradients produce a compression of the acoustics medium and pressure gradients are related to acceleration. Thus, if the dependent variable is, *e.g.*, the acoustic pressure, then the Neumann boundary condition (5) represents a prescribed velocity distribution on that portion of the wet surface, where h is proportional to the velocity and the presence of ik is a consequence of differentiation with respect to time. Neumann boundary conditions are therefore very common in physical situations that entail *radiation*, and in the model problems and demonstrative examples that are subsequently considered we emphasize boundary conditions of this type. It should be noted that the analysis is valid for any combination of boundary conditions on the wet surface for the boundary-value problem (3)-(6), and by no means is it limited to Neumann problems. For *scattering* problems, a fixed rigid object is represented by a homogeneous Neumann boundary condition, often referred to as a hard scatter. Conversely, the homogeneous Dirichlet boudary condition, an appropriate representation of a site of pressure release, is termed a soft scatter. An impedance boundary condition is a linear combination of the two.

3.BURTON AND MILLER FORMULATION FOR EXTERIOR ACOUSTICS PROBLEMS USING DUAL BEM

The governing equation for an exterior acoustics problem is the Helmholtz equation shown in Eq.(3), where f in Eq.(3) is zero (no sources). The boundary conditions can be either the Neumann or Dirichlet type. Based on the dual formulation, the dual equations for the boundary points are

$$\pi u(x) = C.P.V. \int_B T(s,x)u(s)dB(s) - R.P.V. \int_B U(s,x)t(s)dB(s),\ x \in B \quad (7)$$

$$\pi t(x) = H.P.V. \int_B M(s,x)u(s)dB(s) - C.P.V. \int_B L(s,x)t(s)dB(s),\ x \in B \quad (8)$$

where *C.P.V.*, *R.P.V.* and *H.P.V.* denote the Cauchy principal value, the Riemann principal value and the Hadamard principal value, $t(s) = \frac{\partial u(s)}{\partial n_s}$, B denotes the boundary enclosing D and the explicit forms of the four kernels, U, T, L and M, can be found in [10]. The linear algebraic equations discretized from the dual boundary integral equations can be written as

$$[T_{pq}]\{u_q\} = [U_{pq}]\{t_q\} \quad (9)$$

$$[M_{pq}]\{u_q\} = [L_{pq}]\{t_q\}, \quad (10)$$

where $\{u_q\}$ and $\{t_q\}$ are the boundary potential and flux, and the subscripts p and q correspond to the labels of the collocation element and integration element, respectively. The influence coefficients of the four square matrices $[U], [T], [L]$ and $[M]$ can be represented as

$$U_{pq} = R.P.V. \int_{B_q} U(s_q, x_p)dB(s_q) \quad (11)$$

$$T_{pq} = -\pi\delta_{pq} + C.P.V. \int_{B_q} T(s_q, x_p)dB(s_q) \quad (12)$$

$$L_{pq} = \pi\delta_{pq} + C.P.V. \int_{B_q} L(s_q, x_p)dB(s_q) \quad (13)$$

$$M_{pq} = H.P.V. \int_{B_q} M(s_q, x_p)dB(s_q), \quad (14)$$

where B_q denotes the q^{th} element and $\delta_{pq} = 1$ if $p = q$; otherwise it is zero. In order to avoid the problem of fictitious frequency, the Burton and Miller formulation [8] is employed by combining the dual equations as follows,

$$\{[T_{pq}] + \frac{i}{k}[M_{pq}]\}\{u_q\} = \{[U_{pq}] + \frac{i}{k}[L_{pq}]\}\{t_q\} \quad (15)$$

For all wave numbers, Eq.(15) can work well.

4. ERROR INDICATORS USING THE DUAL BEM

Based on the Burton and Miller formulation, the exterior acoustics problems can be solved for all wave numbers. By substituting the solved boundary unknowns in Eq.(15) into Eg.(7) and Eq.(8), we have the two residuals for error indicators,

$$\varepsilon_{UT} = -\pi u(x) + C.P.V. \int_B T(s,x)u(s)dB(s) - R.P.V. \int_B U(s,x)t(s)dB(s),\ x \in B \quad (16)$$

$$\varepsilon_{LM} = -\pi t(x) + H.P.V. \int_B M(s,x)u(s)dB(s) - C.P.V. \int_B L(s,x)t(s)dB(s),\ x \in B \quad (17)$$

Theoretically, ε_{UT} and ε_{LM} in Eqs.(16) and (17) are both zeros if no numerical error is involved. In real calculations, the two residuals are not zeros when collocating points along the boundary as shown below

$$\{\varepsilon_{UT}\} = [T_{pq}]\{u_q\} - [U_{pq}]\{t_q\} \quad (18)$$

$$\{\varepsilon_{LM}\} = [M_{pq}]\{u_q\} - [L_{pq}]\{t_q\}, \quad (19)$$

The two values are the important information for the error indicators. If the exact solution is available, the third error indicator along the boundary can be defined as

$$\varepsilon_{ex} = \mid u - u_e \mid, \quad (20)$$

and

$$\varepsilon_{ex} = \mid t - t_e \mid \quad (21)$$

for the Neumann and Dirichlet problems, respectively.

5. ADAPTIVE SCHEME IN DUAL BEM

The role of the adaptive tactical procedure is to determine the region where the elements should be refined. This algorithm is very strongly dependent on error estimation and the mesh refinement scheme. The reference value, error convergency and equilibrium criterion methods have been popular adaptive tactics for the h-refinement scheme. In the case of the reference value method, elements are refined when their errors are larger than the prescribed reference value. Denoting the error at the ith element by ε_i, the reference value $\bar{\varepsilon}$ may be defined as

$$\bar{\varepsilon} = \text{Average of } \varepsilon_i \quad (22)$$

or

$$\bar{\varepsilon} = \eta \times max(\varepsilon_i) \ \ (0 < \eta < 1). \quad (23)$$

In this paper, the former value in Eq.(22) is chosen because it is difficult to specify the value of η in Eq.(23) adequately.

Since the error estimator and adaptive tactics can be obtained, the self adaptive mesh refinement process can be implemented. The flowchart of the self adaptive mesh refinement is shown in Fig.2. Fig.2 provides a simple illustration of how adaptive BEM works; all adaptive computations fit mor or less into this general framework. The flowchart shows how the various components of adaptivity works together to put the efficient elements in the meshes. Then a posteriori error estimator takes the Burton and Miller boundary solution as input and computes an estimate of the solution error by using the dual BEM. According to the estimated error distribution, a new, more efficient mesh can be constructed. The mesh generator then creates the adaptive mesh with the requested size distribution, and the process repeats until a stopping criterion is satisfied. The coarse mesh is initiated in the beginning, and drive the adaptive refinement through the selection of smaller and smaller error tolerance in the iteration. Usually, three or four iterations are sufficient. Efficiency is attained by placing more elements in areas where errors are large. In doing so, the adaptive strategy attemps to compute a distribution of element size such that the error is equidistributed among the elements in the mesh. Based on the reference value method for the self adaptive technique, the minimum number of elements can be obtained under the requirement of error tolerance. Thus, the measure of error must be specified. Although many measures of error have been used, *e.g.*, (a). Pointwise error, (b). Max norm: $\|u - u_e\| = max_{a \le x \le b} |u(x) - u_e(x)|$, (c). L_2 norm: $\|u - u_e\| = \{\int_a^b |u - u_e|^2 dx\}$, and (d). Energy norm: $\|u - u_e\| = \{\int_a^b \sum_{i=0}^m |\frac{du}{dx} - \frac{du_e}{dx}| dx\}^{\frac{1}{2}}$, the L_2 norm along the boundary in the energy sense has been adopted in this paper.

6. NUMERICAL EXAMPLES

Case 1: Nonuniform radiation problem by a cylinder (Neumann boundary condition)

The problem was chosen because the exact solution is known [11]. It is therefore a good model problem to test the effectiveness of the error estimator and adaptive strategy since the solution is directional and effect of adaptivity may be significant. The example with the Neumann boundary condition is shown in Fig.3. The analytical solution is

$$u(r,\theta) = \frac{2}{\pi} \sum_{n=0}^{\infty}{}' \frac{-1}{k} \frac{sin(n\alpha)}{n} \frac{H_n^{(1)}(kr)}{H_n^{(1)\prime}(ka)} cos(n\theta). \quad (24)$$

where $'$ is the Neumann factor. The contour plots for the real-part solutions are shown in Fig.4 for the case of $\alpha = \frac{\pi}{9}$. It indicates that numerical results agree well with the analytical solution. Also, it is interesting to find that the irregular frequencies in Fig.5 occurs as predicted theoretically by Chen and Kuo [9]. This confirms the conclusion in [9] that the irregular frequencies depend on the integral formulation (UT or LM method) instead of the types

of boundary conditions (Dirichlet or Neumann). For the case of $ka = 1$, we can construct the three error tracking curves in Fig.6(a) for the initial mesh. Burton and Miller method can work well for all wave numbers and the UT and LM results agree well except at the irregular wave numbers as shown in Fig.5. It is found that irregular values occur at J_n^m, the mth zeros of $J_n(ka)$ for the UT formulation, while the LM formulation has the irregular values of $J_n'^m$, the mth zeros of $J_n'(ka) = 0$. According to the adaptive scheme, meshes of twelve, twenty and twenty-eight elements are successively created in Fig.7. The high density of mesh near the boundary with discontinuous potential is found in a consistent way of engineering judgement. The successive error tracking curves are also constructed in Figs.6(b), (c) and (d). The convergence rate using the adaptive mesh is faster than the uniform meshes does as shown in Fig.8.

Case 2: Scattering problem by a square rod (Neumann boundary condition)
Having demonstrated the adaptive technology on the infinite circular cylinder, we proceed to a problem in which exact solution is not available [7]. Due to nonsmooth boundary of four corners in the square, the scattering by the infinite square rod of area $4m^2$ is more directional and thus leads itself more to adaptivity. According to the adaptive scheme, meshes of twelve, twenty and twenty-eight elements are successively created in Fig.9. Solution contours of $Re(u)$ for $ka = 4\pi$ are shown in Fig.10. In Fig.11, the real and imaginary components of u on the radius $r = \frac{1}{0.425}$ is plotted for comparison with DtN FEM results. Solutions of the initial mesh and the successive meshes are compared. The convergence rate using daptive mesh is faster than that using the uniform mesh.

7. CONCLUSIONS

In this paper, we demonstrated boundary element solution – adaptive acoustics methodologies on model time-harmonic exterior acoustics problems in two dimensions. The results indicate that adaptivity can provide an increase in mesh efficiency for the Helmholtz problems at moderate wave numbers. The adaptive computations involved the Burton and Miller formulation and the dual BEM. Three error tracking curves were constructed and behaved consistently. According to the error tracking curves, adaptive strategy can be implemented. Based on the posterior pointwise error distribution, adaptive mesh was generated to speed up the convergence rate in comparison with uniform mesh.

Acknowledgements

The authors thank to Mr. C. T. Chen who prepared some numerical results. Also, the finiacial supprot from NSC projects with Grants Number NSC 89-2211-E-019-003 and NSC 89-2211-E-019-022 is highly appreciated.

References

[1]Kita, E. & Kamiya, N. Recent studies on adaptive boundary element methods. *Advances in Engineering Software*, 1994, **19**, 21-32.

[2]Kamiya, N. Aikawa, Y. & Kawaguchi, K. Adaptive boundary element for the problem with mixed boundary condition. *Boundary Elements XVII*, ed. Brebbia C. A., Kim S., Osswald T. A. & Power H., 1995.

[3]Zarikian, V. Gray, L. J. & Paulino, G. H. Pointwise error estimates for boundary element calculations. *Boundary Element Technology IV*, ed. by Brebbia, C. A. & Kassab, A. J. Computational Mechanics Publications, 1994, 253-260.

[4]Paulino, G. H. Gray, L. J. & Zarikian, V. *A posteriori* pointwise error estimates for the boundary element method. Oak Ridge National Laboratory, ORNL/TM-12820, 1995.

[5]M. T. Liang, J. T. Chen, S. S. Yang Error estimation for boundary element method. *Engineering Analysis with Boundary Elements*, 1999, **23**, 257-265.

[6]Harari, I., Barbone, P. E., Slavutin, M. and Shalom, R., Boundary Infinite Elements for the Helmholtz Equation in Exterior Domains, *Int. J. Numer. Meth. Engng.*, 41, pp.1105-1131, 1998.

[7]Stewart, J. R., Hughes, T. J. R., *h*-Adaptive Finite Element compution of time-harmonic exterior accoustics problems in two dimension, *Computer Methods Appl. Mech. Engng.*, 146, pp.65-89, 1997.

[8]Burton, A. J. and Miller, G. F., The Application of Integral Equation Methods to Numerical Solution of

Some Exterior Boundary Value Problems, *Proc. R. Soc. London Ser. A*, 323, pp.201-210, 1971.

[9] Chen, J. T. and Kuo, S. R., On fitious freguencies using circulants for radiation problems of a cylinder,*Mech. Res. Comm.*, 27, pp.49-58, 2000.

[10] Chen, J. T. and Chen, K. H., Dual integral formulation for determining the acoustic modes of a two-dimensional cavity with a degenerate boundary, it Engng. Anal. Bound. Elem., 21, pp.105-116, 1998.

[11] Harari, I., Barbone, P. E., Slavutin, M. and Shalom, R., Boundary Infinite Elements for the Helmholtz Equation in Exterior Domains, *Int. J. Numer. Meth. Engng.*, 41, pp.1105-1131, 1998.

[12] Chen, J. T., Chen, C. T., Chen, K. H., Chen, I. L., On fictitious frequencies using dual BEM for nouniform radiation problems of a cylinder, *Mechanics Research communications*, Accepted, 2000.

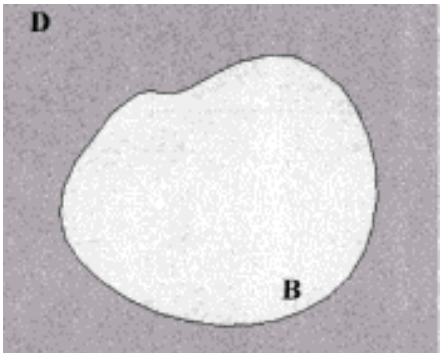

Fig1(a) An unbounded domain with a smooth internal boundary.

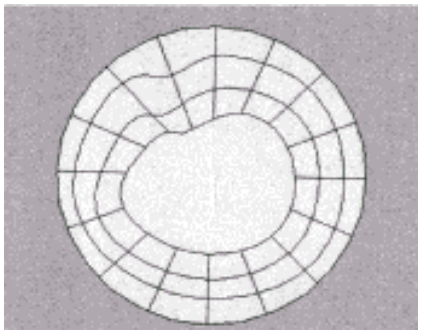

Fig1(b) DtN FEM mesh.

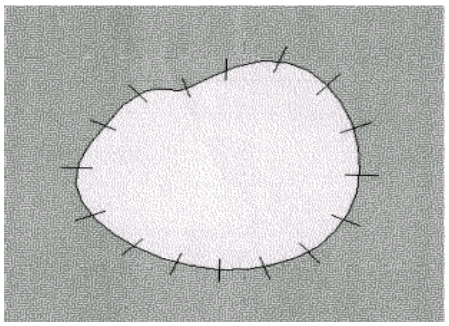

Fig1(c) BEM mesh.

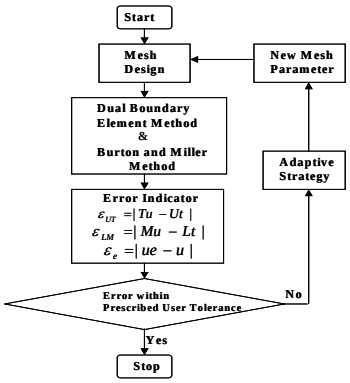

Fig.2 Flowchart of adaptive mesh generation.

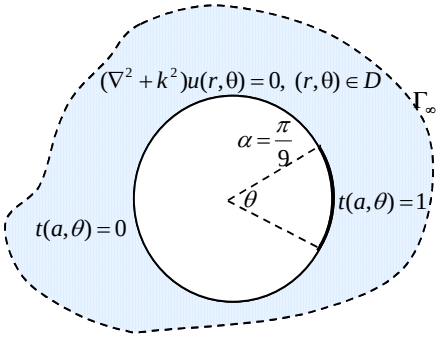

Fig.3 The onuniform radiation problem (Neumann condition) for a cylinder.

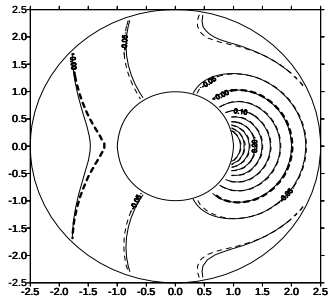

Fig.4 The contour plot for the real-part solutions (analytical solution: dashed line, numerical result: solid line).

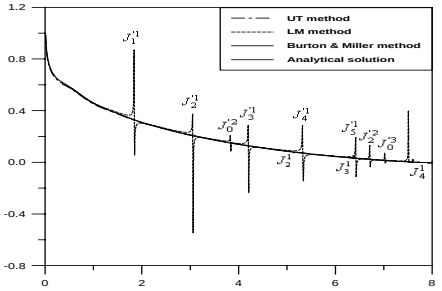

Fig.5 The positions of irregular values using different methods.

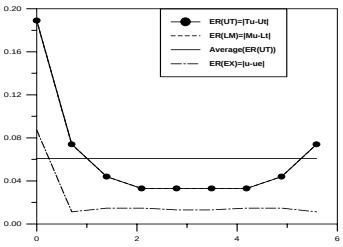

Fig.6(a) Error tracking curve (9 elements).

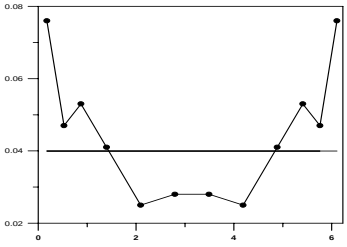

Fig.6(b) Error tracking curve (12 elements).

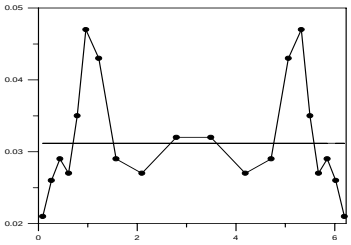

Fig.6(c) Error tracking curves (20 elements).

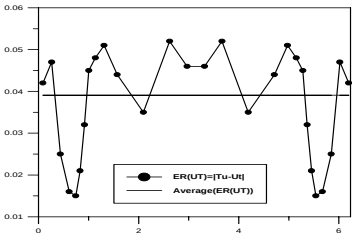

Fig.6(d) Error tracking curves (28 elements).

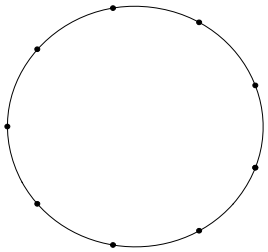

Fig.7(a) Adaptive mesh (9 elements).

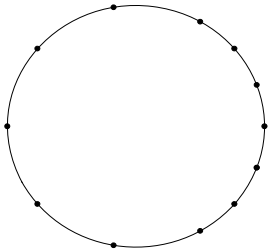

Fig.7(b) Adaptive mesh (12 elements).

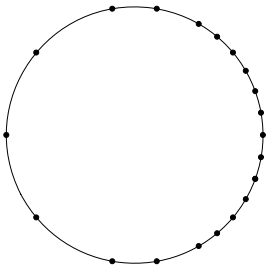

Fig.6(c) Adaptive mesh (20 elements).

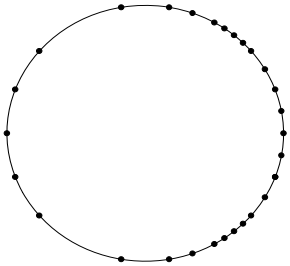

Fig.7(d) Adaptive mesh (28 elements).

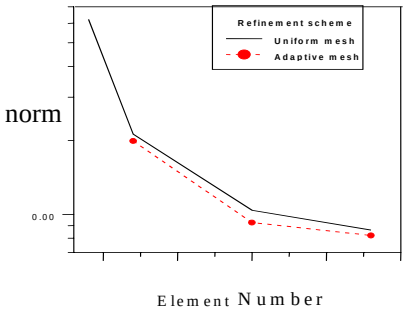

Fig.8 Convergence rate using uniform mesh and adaptive mesh.

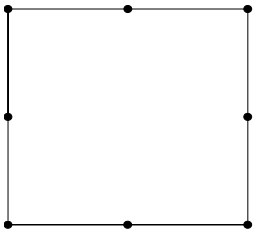

Fig.9(a) Adaptive meshes (8 elements).

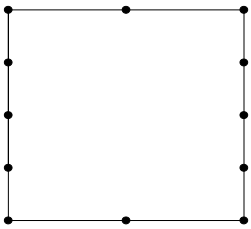

Fig.9(b) Adaptive meshes (12 elements).

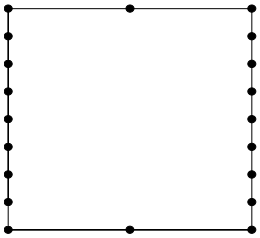

Fig.9(c) Adaptive meshes (20 elements).

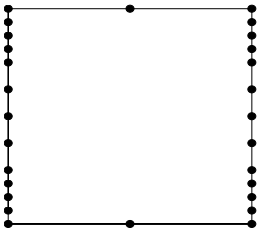

Fig.9(d) Adaptive meshes (28 elements).

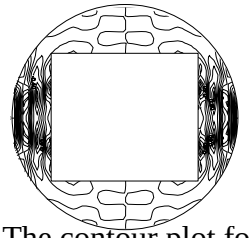

Fig.10(a) The contour plot for the real-part solutions (8 elements).

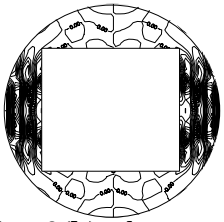

Fig.10(b) The contour plot for the real-part solutions (12 elements).

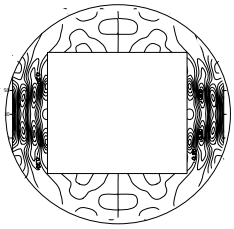

Fig.10(c) The contour plot for the real-part solutions (20 elements).

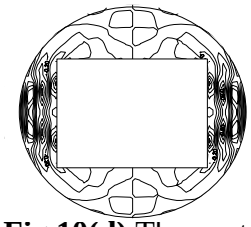

Fig.10(d) The contour plot for the real-part solutions (28 elements).

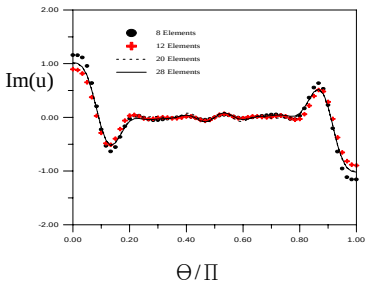

Fig.11(a) Plane scattering by an infinite square rod, 4π, imaginary part of solution at r=1/0.425 (only the top of the boundary is plotted).

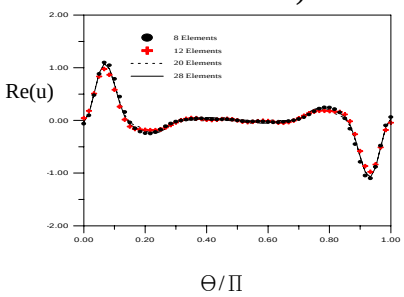

Fig.11(b) Plane scattering by an infinite square rod, 4π, real part of solution at r=1/0.425 (only the top of the boundary is plotted).